Molecular Dynamics Simulation of Nucleation in the Freezing of Molten Potassium Iodide Clusters

Jinfan Huang and Lawrence S. Bartell*

Department of Chemistry, University of Michigan, Ann Arbor, Michigan 48109

Received: November 15, 2001; In Final Form: January 15, 2002

Molecular dynamics simulations have been carried out to study the effects of cluster size and temperature on the nucleation rate in potassium iodide clusters in the temperature range of 400−580 K. The clusters $(KI)_{108}$, $(KI)_{256}$, and $(KI)_{500}$ were studied. The rate at which nuclei materialized per unit volume appeared to decrease with increasing cluster size. This size dependence could be accounted for by the agency of three roughly equal factors, namely, the Laplace pressure, the larger coefficients of diffusion for the smaller clusters, and the area-to-volume ratio. The latter factor arises because nucleation invariably occurs at the surface rather than in the interior of the clusters. Sizes of critical nuclei obtained by direct counting of ordered molecules were considerably larger than predicted by the classical nucleation theory unless the outer layer of ordered molecules was subtracted from the total count. The rationale for such a subtraction is that the outer layer corresponds to the ordered liquid layer predicted by Turnbull. Consistent with Kashchiev's criterion, the number of nuclei per cluster increased with cluster size and with increased supercooling. Nucleation time lags decreased as the degree of supercooling increased. The temperature dependence of the kinetic parameters of the interfacial free energy between the solid and the liquid and the Granasy interface thickness derived from the nucleation rates are discussed. A pictorial account of nucleation and subsequent crystal growth in a typical $(KI)_{500}$ cluster is presented.

I. Introduction

In our current experimental and computational program of research on the nucleation[1−4] of crystals in the freezing of various types of liquids including molecular, metallic, and ionic systems, we broaden our study of salts to include another alkali halide. Alkali halides are among the simplest ionic substances and are widely used as optical materials. The study of nucleation and crystallization in such materials is of potential value for both science and technology. Nucleation in the freezing of alkali halides was studied previously in a high-temperature cloud chamber by Buckle and Ubbelohde.[5,6] Our prior studies of salts included studies of clusters of NaCl[7,8] and RbCl.[9,10] In this paper, we report the results of molecular dynamics (MD) simulations of the highly supercooled clusters $(KI)_{108}$, $(KI)_{256}$, and $(KI)_{500}$ in the temperature range of 400−580 K. Such supercooling is much deeper than that encountered in conventional nucleation experiments.

II. Procedure

Computational Details. Molecular dynamics simulations were performed with a modified version of the program MDIONS[11] in which the leap-frog algorithm was used to propagate the evolution of the systems. The configurational energy of an ionic cluster with the rock-salt structure depends greatly on the cluster's external shape. The external shape for which the configuration energy is lowest is that of a cube, consistent with the structure easily observed in table salt with the aid of a magnifying glass. Therefore, clusters were constructed to have cubic shapes for the starting points in all runs. The initial configuration was based on a face-centered-cubic (fcc) cell with a cell constant of 7.052 Å, the value observed in the bulk material at 301 K.[12] Initial starting configurations were constructed by stacking unit cells into arrays with edge lengths corresponding to 3, 4, and 5 cells, yielding the clusters $(KI)_{108}$, $(KI)_{256}$, and $(KI)_{500}$, respectively.

TABLE 1: Potential Parameters for KI Adopted for the Simulation

	K^+-K^+	K^+-I^-	I^-I^-
A (J/molecule)	4.255×10^{-20}	3.380×10^{-20}	2.535×10^{-20}
σ (Å)	2.926	3.370	3.814

The interaction potential used was of the Born−Mayer−Huggins[13−16] type

$$U = \Sigma\{q_i q_j r_{ij}^{-1} + A_{ij} \exp[(\sigma_{ij} - r_{ij})/\rho]\} \qquad (1)$$

consisting of a simple Coulomb interaction plus a short-range repulsive interaction. Here, q_i and q_j are the charges on ions i and j, respectively, and r_{ij} represents the distance between ions i and j. The values of the KI parameters A_{ij} and σ_{ij} listed in Table 1 were taken from Tosi and Fumi,[16] as was the constant $\rho = 0.355$ Å.

Simulations for all clusters began with 5000 time steps spent in a bath at 298.15 K, followed by another 5000 time steps at constant energy and then another 5000 time steps in the bath, followed by 10 000 time steps at constant energy. In all of the simulations, the time steps were set at 8 fs. In stages spent in the heat bath, the temperature fluctuation was limited to ±4 K. Velocity rescaling was performed whenever the temperature difference between the system and the bath exceeded that limit. Heating stages then began at 320 K, with each succeeding stage 20 K warmer than the previous one. Every stage was first run at constant temperature (±4 K) for 5000 time steps and then for 5000 time steps at constant energy. Heating was continued to 1040 K, which is approximately 85 K above the melting point

10.1021/jp0142381 CCC: $22.00 © 2002 American Chemical Society
Published on Web 02/16/2002

TABLE 2: Nucleation Rates ($m^{-3}s^{-1}$) $\times 10^{-35}$, Raw and Corrected[a] with Statistical Uncertainties, and Average Number of Critical Nuclei, $\langle N \rangle$, Per Cluster

cluster		400 K	450 K	500 K	550 K	580 K
$(KI)_{108}$	*J*, raw	37	26	17(5)		
	J, corr	35(11)	27(9)	18.5(6)		
	$\langle N \rangle$	~1.25	~1.12	1.06		
$(KI)_{256}$	*J*, raw			10	5.7	
	J, corr			7(2)	5(2)	
	$\langle N \rangle$			1.81	1.38	
$(KI)_{500}$	*J*, raw			7.3	3.9	1.2
	J, corr			4.4(1.4)	3.0(1)	1.2(0.4)
	$\langle N \rangle$			2.25	1.89	1.18

[a] See text.

of the bulk and, hence, even higher above the melting points of the clusters. Such heating left the resultant molten droplets with no detectable crystalline nuclei, certainly none remotely approaching the critical size. Melting points were inferred from caloric curves.

Freezing was carried out by reversing the stages of the melting process. Melted clusters were cooled through a series of stages starting from 850, 980, and 1040 K for $(KI)_{108}$, $(KI)_{256}$, and $(KI)_{500}$ respectively, with each succeeding stage 20 K cooler than the previous one, until the clusters reached 320 K. Therefore, heating/cooling rates were 2.5×10^{11} K/s.

Nucleation was studied in a different series of runs from the freezing runs described above. Rates were based on 16 nucleation events for each cluster size at each temperature listed in Table 2. Clusters with different thermal histories were generated as follows. For the $(KI)_{108}$ cluster which was thoroughly melted at 850 K, the configuration obtained in the heating stage described above was additionally annealed in a bath at 850 K for 5000 time steps, followed by another 5000 time steps at constant energy, and then another 32 000 time steps in the heat bath. After every 2000 time steps, the configuration was saved, thereby generating 16 independent clusters for freezing runs. For the larger clusters, the same procedure was followed, except that the 16 independent $(KI)_{256}$ clusters were generated at 980 K, whereas those for $(KI)_{500}$ were generated at 1040 K. The reason for choosing different temperatures for the different cluster sizes was to ensure that the clusters were completely melted and, at the same time, that no evaporation had taken place. At the temperatures at which the independent configurations were generated, no solid nuclei remained according to the diagnostic test to be described subsequently.

Nucleation rates were investigated by immediately quenching the melted clusters in a heat bath at the temperature of interest. The first temperature for nucleation runs on $(KI)_{108}$ clusters was chosen to be 500 K, namely, the highest temperature at which nucleation occurred during our simulation times. At this temperature and below, the $(KI)_{256}$ and $(KI)_{500}$ clusters readily froze, often into polycrystalline solids. The highest temperature for $(KI)_{256}$ was chosen to be 550 K for the same reason, and that for $(KI)_{500}$ to be 580 K. Two additional temperatures, 400 and 450 K, were added for $(KI)_{108}$ clusters to extend the temperature range in this study.

Diagnosis of Melting and Freezing. In our previous simulations of salt clusters, various diagnostic tests were applied during the heating and cooling processes to monitor the behavior of the ions.[7] Melting and freezing were followed by observing the temperature dependencies of the caloric curve, the Lindemann index δ, and the pair correlation function. All three criteria gave virtually the same melting points. Therefore, in the present study, only the caloric curves were used for this purpose. The proprietary program MACSPIN offers a very convenient way to view images of the arrangements of ions and to follow the progress of a phase change. This monitoring is especially useful in identifying how many solid nuclei form and where they form in a cluster, in monitoring the crystal growth, and in judging whether the final solid cluster is a single crystal or is polycrystalline. Sometimes, two separate nuclei jostle against each other and readjust, and they may merge into a single crystal.

In a previous paper, we proposed a simple method for identifying solidlike nuclei. The model criterion for solidlike aggregates requires the coordination number to be 12 (within a cutoff distance corresponding to the first minimum of the pair-correlation function of cation−cation or anion−anion pairs).[7,8] An ion with such a coordination number is considered to be "crystalline", i.e., in a crystalline environment. Such a method, although very simple, yields results closely similar to those of other criteria based on Voronoi polyhedra and "bond-order" values adopted in this laboratory for molecular clusters.[17,18] This procedure is quite effective in recognizing the sharp increase in the size of a solidlike nucleus that corresponds to the onset of nucleation. We apply this simple method in the present work without further modification and refer to each center with a coordination number of 12 as an "fcc unit".

Estimation of Nucleation Rate. If the fraction of unfrozen clusters obeys a first-order rate law, the expression

$$\ln[N_n(t_n)/N_o] = -JV_c(t_n - t_o) \tag{2}$$

will hold, where N_o is the total number of clusters; $N_n(t_n)$ is the number of clusters containing no critical nuclei just before the nth nucleation event at time t_n, or[19]

$$N_n(t_n) = N_o - n + 1 \tag{3}$$

J is the nucleation rate; V_c is the volume per cluster; and t_o is the time lag to achieve a steady state of formation of nuclei. The limiting slope of the curve $\ln[N_n(t_n)/N_o]$ vs t_n yields an estimate of J, the nucleation rate of freezing, and the intercept gives the time lag. The times t_n are estimated from the sharp increase in the numbers of fcc units described in the previous section. Because of the stochastic nature of the nucleation events, appreciable statistical uncertainties arise when N_o is small. To help optimize the analysis, a weighted least-squares procedure was carried out to determine J and t_o. Details are outlined in ref 19.

Corrections need to be applied to the values of J and t_o so derived. Nucleation rates and time lags derived from times of onset of nucleation by applying eq 2 neglect the phenomenon of transient nucleation. According to this phenomenon, the quantity $\ln(N/N_o)$ increases smoothly from zero at early times instead of remaining zero until time t_o is encountered. Therefore, both the nucleation rate and the time lag derived from the linear fit via eq 2 tend to be too small. In a forthcoming paper, the correction for this neglect is described in detail.[20]

Also to be treated in this paper is a method for correcting nucleation rates when multiple nucleation events occur in the larger clusters but only the time of the first nucleation event is recorded. This selection of onset times biases the nucleation times to be too small in the case of polynuclear freezing. Values in Table 2 are corrected both for polynuclear freezing and for the effect of transient nucleation, assuming that the relevant Wu moment M[21] corresponds to the value inferred from transient nucleation computations by Greer and Kelton,[21] so that $2M/t_o^2$ is about 1.2. A value of unity for this quantity would correspond exactly to eq 2.

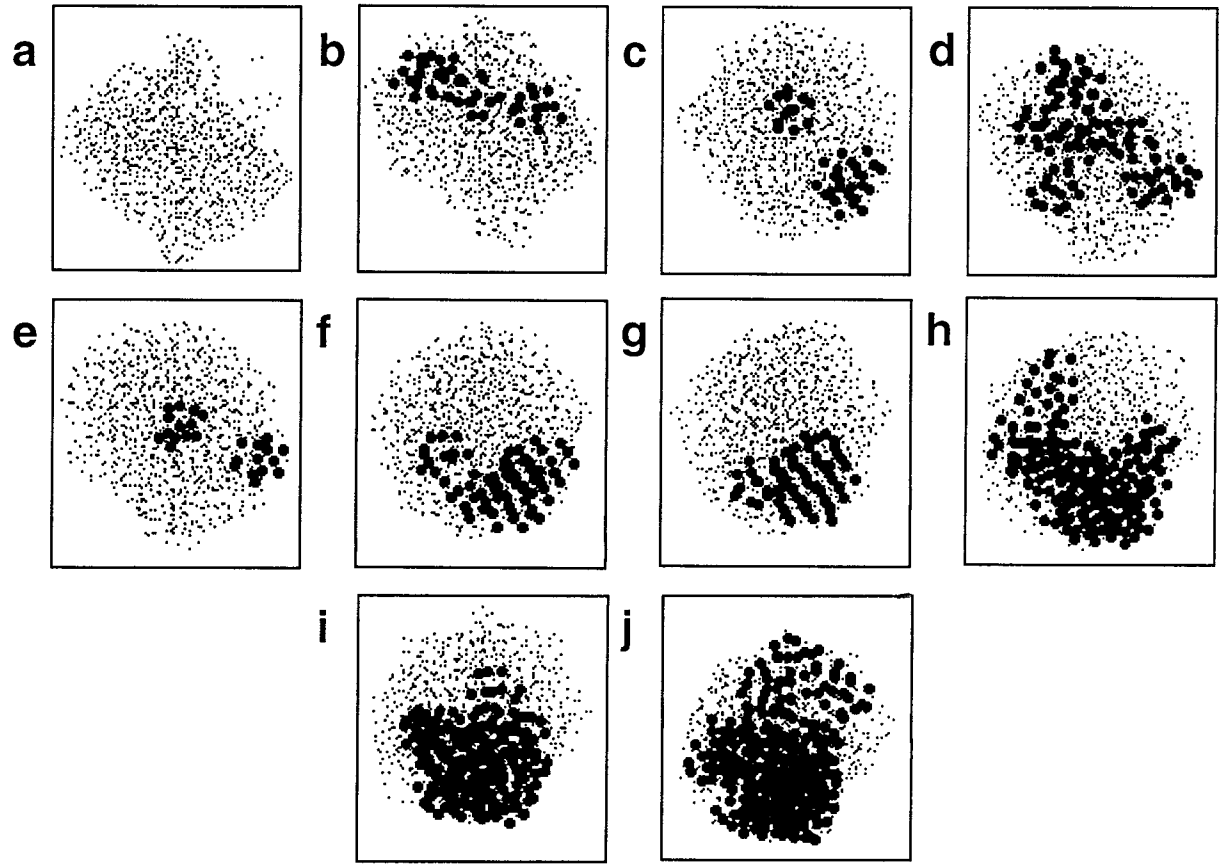

Figure 1. Images of a $(KI)_{500}$ cluster at various stages after having been quenched from 1040 K in a 580-K heat bath. Times in picoseconds after immersion in the bath: (a) 0.8, (b) 24, (c) 36, (d) 72, (e) 76, (f) 81, (g) 146, (h) 156, (i) 172, (j) 180.

TABLE 3: Nucleation Time Lags (ps), Corrected for Transient Nucleation, with Statistical Uncertainties

cluster	400 K	450 K	500 K	550 K	580 K
$(KI)_{108}$	11(2)	18.5(4)	40(9)		
$(KI)_{256}$			12(3)	32(7)	
$(KI)_{500}$			26(6)	46(10)	71(16)

Estimation of Interfacial Properties. For homogeneous nucleation, the rate can be expressed by[23,24]

$$J(T) = A \exp(-\Delta G^*/k_B T) \quad (4)$$

where ΔG^* is the free energy barrier to the formation of a critical nucleus from the liquid. Procedures for deriving the interfacial free energy σ_{sl} from ΔG^* via the classical nucleation theory (CNT), and the interfacial thickness δ associated with the diffuse-interface theory (DIT),[25−29] are outlined in the Appendix. Because of the uncertainties in the temperature-dependent heat capacities, quantities that enter the analyses, as a compromise, we adopted a mean value of 15.4 J K^{-1} mol^{-1} for ΔC_p. Because some of the properties adopted (see Appendix) are from the bulk material while others are from the simulations themselves, the derivations of σ_{sl} and δ are not fully rigorous.

III. Results

Nucleation rates of clusters of different sizes at different temperatures are summarized in Table 2. Table 3 reports the nucleation time lags found in the simulations. Listed in Table 4 are the interfacial free energy and the diffuse-interface thickness parameters derived from the nucleation rates given in Table 2 by applying the classical nucleation theory[24] and the diffuse-interface theory.[25−29]

TABLE 4: Interfacial Free Energy and Diffuse Interface Thickness Parameters Derived from MD Simulations[a]

	400 K		450 K		500 K		550 K		580 K	
cluster	σ_{sl}	δ	σ_{sl}	δ	σ_{sl}	δ	σ_{sl}	δ	σ_{sl}	δ
$(KI)_{108}$	41	3.0	44	2.7	46	2.4				
$(KI)_{256}$					46	2.3	46	2.3		
$(KI)_{500}$					46	2.3	47	2.1	48	2.0

[a] σ_{sl} is in mJ/m^2; δ is in Å.

Selected cluster images generated from the MACSPIN program are shown in Figure 1. They illustrate the evolution of structural changes when a completely melted $(KI)_{500}$ cluster is put into a heat bath at 580 K. Both nucleation events and crystal growth can be seen. Precritical nuclei form and disappear until a concerted growth eventuates.

IV. Discussion

Nucleation Time Lags. For each cluster size, the period of transient nucleation shortens as the drive to nucleate is enhanced by increasing supercooling. This is not the trend often found (see refs 1 and 30). In the well-known treatments of time lag by Kashchiev, Collins, Wakeshima, and Chakraverty summarized by Kelton, Greer, and Thompson,[30] the most important factor determining the time lag is $(n^*)^3 T/D\Delta G_{fus}$, where n^* is the number of molecules in the critical nucleus. In typical systems, the precipitous decrease in the coefficient of diffusion D as supercooling deepens overbalances the changes in the other terms. In the present case, however, calculations based on the CNT and entries in Table 6 suggest the opposite trend for potassium iodide, consistent with observations from the MD runs. At temperatures below 400 K, the rapid drop of D appears

TABLE 5: Quantities Contributing to the Size Effect on Nucleaton Rate

source\cluster	$(KI)_{500}$	$(KI)_{256}$	$(KI)_{108}$
w'	(1)	1.3	2.0
D	(1)	1.2	1.75
surface/volume	(1)	1.25	1.67
observed	(1)	1.6(0.7)	4.1(1.8)

to reverse the trend. Not understood in the MD results is the variation in time lags for the different cluster sizes. In a prior paper from this laboratory,[18] evidence was cited that indicated that the free energy of freezing per unit volume of very small clusters tends to be smaller in magnitude than that in larger clusters, a plausible situation for $(KI)_{108}$, which was found to have an extremely diffuse surface.[31] This would accord with the larger time lag in comparison with those of the larger clusters.

Polynuclear Freezing. Kashchiev[32] has proposed a criterion for whether multiple nucleation events, or only a single event, occur in a given volume. Applied to clusters, the criterion to guarantee that the freezing is mononuclear is for the ratio $G/JV_c^{4/3}$ to be considerably greater than unity, where G is the linear growth rate. Therefore, the larger the cluster, the more likely that freezing is polynuclear. More interesting is the temperature effect. For a given cluster size, the growth rate tends to increase as the temperature increases, whereas the nucleation rate decreases, favoring mononuclear freezing. As shown in Table 2, these trends for the average number of nuclei per cluster are exhibited in the MD simulations.

Size Dependence of Nucleation Rate. Although the statistical uncertainty in the nucleation rates is fairly large, two consistent trends can be seen in the data. First, the nucleation rates increase as the degree of supercooling increases. Such behavior is expected from nucleation theory until further cooling increases the viscosity of the liquid so greatly that the decreasing mobility of the ions hinders the transformation. More noteworthy is the consistent increase in rates with decreasing cluster size. Although there are a number of size-dependent quantities in the terms that enter nucleation theory, three stand out in particular. These are the Laplace pressure entering the term w' (see Appendix, eq 11), the greater coefficient of diffusion in the smaller clusters, and the tendency for nucleation to occur at or very near the surface of clusters. Another potential source is the size dependence of the difference between heat capacities of the solid and liquid, which determines the free energy of freezing of supercooled droplets. Although the noise in the MD data makes this difference very uncertain, it appears to be small and to act in a direction opposite to the observed effect on nucleation rates

Before estimating the magnitudes of the factors mentioned above, a brief discussion of the corrections to the nucleation rates calculated by incorrectly assuming the freezing to be mononuclear should be made. Because it is relatively easy to recognize the time of the first nucleation event but less simple to identify times of later events, our custom has been to record only the time of the first nucleation event in a cluster. This bias in nucleation times[20] is corrected in the nucleation rates and time lags listed in Tables 2 and 3.

Fortunately, it is possible to obtain rough estimates of the magnitudes of the size effects enumerated above. Let us consider the first effect. For a liquid cluster, a crude estimate of the Laplace pressure, $2\sigma_{lv}/R$, is possible, where R is the radius of the cluster. In the case of many small liquid drops in the size range of the present KI clusters, the effect of Tolman's delta in lowering the surface tension σ_{lv} is almost negligible, so we ignore it. In ref 31, however, we show that the boundaries of small KI clusters are very diffuse, so diffuse, in fact, that it is not clear that the surface tension inferred for large systems is accurately applicable, nor is it clear what radius should be applied. Moreover, the observed tendency of nuclei to form at the surface instead of in the interior of a cluster makes the rationale for w' somewhat speculative. Nevertheless, the general order of magnitude of the effect of the Laplace pressure can be estimated if we neglect these complications. Thus, for example, for $(KI)_{108}$ at 500 K, the Laplace pressure is roughly 1500 atm. Such a pressure can have a substantial effect. This effect of pressure is greater according to the DIT than it is according to the CNT.[19]

The effect of coefficient of diffusion, D, is more straightforward, as it enters the nucleation prefactor directly. From the coefficients determined in ref 31, we obtain the effect on the nucleation rates. In addition, a crude estimate of the effect arising from the fact that nucleation tends to occur at the surface can be made. By convention, nucleation rates are calculated on the basis of nuclei per unit time per unit volume. If it is assumed that the rate more nearly reflects the nuclei per unit surface area per unit time and that the molten clusters are spherical, an estimate of the effect can be made from the surface-to-volume ratio of $3/R$. This suggests that enhancement factors for $(KI)_n$ relative to $(KI)_{500}$ would be approximately $(500/n)^{1/3}$. Estimates of effects due to each of the factors, w', D, and surface preference for nucleation are listed in Table 5. Entries in this table indicate that the orders of magnitude of all three factors influencing the size effect on the nucleation rate are comparable, and together, they readily account for the size effects on the rates.

Interfacial Free Energy and the Diffuse Interface Thickness. From the rates of nucleation of the various clusters can be inferred the free energy barrier, ΔG^*, inhibiting nucleation. As shown in the Appendix, this barrier is related to the interfacial free energy parameter σ_{sl} in the CNT and to δ in the DIT, enabling a derivation of these characteristic parameters from the simulations.

For comparison with our results for σ_{sl} in Table 4, a value of 47 mJ/m^2 for KI has been suggested by Buckle and Ubbelohde[6] on the basis of experimental observations of the time required for molten clusters in a heated cloud chamber at 800 K to "twinkle," thereby indicating that freezing was taking place. The authors state that no great accuracy can be claimed, partly because of the uncertainties associated with their theory of time lags and partly because of the "rough-and-ready" estimates of the physical parameters invoked in applying the theory. Nevertheless, it can be seen that their value for their much larger droplets agrees quite well with our values at lower temperatures, which were derived from nucleation rates in simulations, not from time lags.

From the entries in Table 4, it appears that σ_{sl} tends to increase as T increases. If all values for all cluster sizes are taken into account, the increase is roughly proportional to $T^{0.37}$, but if only the more limited data from the larger two clusters are considered, the increase is less steep. Many years ago, Turnbull pointed out that the interfacial excess entropy is negative because the liquid tends to conform to the surface of the crystalline nucleus with which it is in contact and, therefore, to be more ordered than it is far from the surface.[33] If interfacial entropy were an important contribution to the interfacial free energy, it would tend to make σ_{sl} increase with temperature. Turnbull's classic study of the freezing of mercury[34] derived a temperature dependence of T^n with n in the vicinity of 0.3− 0.4, consistent

with the results of this simulation. No other reliable experimental value seems to be available for comparison for any substance. For water, where a larger (20-order-of-magnitude) range of nucleation rates exists, larger than for any other substance, this information would pinpoint n quite effectively if a truly rigorous prefactor were available.[35] It turns out, however, that alternative forms of the prefactor yield quite different values of n.[36]

An empirical relation[37]

$$\sigma_{sl} = k_T \Delta H_{fus}/(V^2 N_A)^{1/3} \quad (5)$$

formulated by Turnbull provides an alternative estimate of the interfacial free energy. In the original paper, the molar volume adopted appears to be that of the liquid near the temperature of the nucleation, but the heat of fusion was that at the freezing point. In recent papers, some authors take ΔH_{fus} to be the value at the nucleation temperature, but we apply that at the freezing point. The proportionality constant k_T was found to be 0.45 for a series of metals but 0.32 for water and a few metalloids.[37] We use the latter result and obtain a value for σ_{sl} of 57 mJ/m^2, a value supposed to apply for shallow supercooling. As noted above, the interfacial free energy appears to increase as the temperature increases. If we adopt the exponent $n = 0.37$ found above from the behavior of all three sizes of clusters and extrapolate the value 46 mJ/m^2 found for all three cluster sizes at 500 K to the melting point, we obtain the result 58 mJ/m^2, in fortuitously good agreement with the value from eq 5.

The interfacial thickness parameter, δ, of Granasy's DIT is supposed to represent the separation of the radius at which the surface excess entropy is zero from the radius at which the surface excess enthalpy is zero. It is not related in any known way to Tolman's δ or to the interface diffuseness. Granasy suggests that the DIT δ is related to the interfacial free energy σ_{sl}^o at the freezing point and the heat of fusion per unit volume of the solid via[25]

$$\delta = \sigma_{sl}^o V_s/\Delta H_{fus} \quad (6)$$

If we apply the value of σ_{sl}^o obtained above by extrapolation of our results at lower temperatures, eq 6 yields $\delta = 1.34$ Å. This result is substantially lower than the MD results in Table 4, although our results suggest a decrease in δ as T increases. Granasy has expressed the belief that his parameter δ is independent of temperature, except for the system of water, on the basis of empirical observations he has made. In the case of water, however, it is necessary to make δ decrease markedly as temperature increases. Although this decrease can readily be rationalized by invoking the two-state model of water, it is possible that other materials also show a decrease of δ with temperature.

Sizes of Critical Nuclei. Images of nuclei materializing in supercooled clusters, as illustrated in Figure 1, are helpful in monitoring the course of nucleation and the growth of nuclei. The size of an individual nucleus at the onset of nucleation can be estimated by identifying the number of contiguous ions satisfying our criterion for ions in ordered, solidlike environments. After examining hundreds of images such as those in Figure 1f and 1g we estimated that the average sizes of critical nuclei in $(KI)_{500}$ were about 35 KI pairs at 500 K, 45 at 550 K, and 60 at 580 K. These numbers are considerably greater than the sizes implied by the capillary theory, according to which the critical size is

$$n^* = (32/3)\pi V_s^2 N_A[\sigma_{sl}/(\Delta G_{fus} - V_s w')]^3 \quad (7)$$

Values of the interfacial free energy derived from the simulations inserted into eq 7 yield 6 KI pairs at 500 K, 7.5 at 550 K, and 9.5 at 580 K. The great disparity between the sizes counted directly from the simulations and the CNT sizes can be put into perspective by noting that Turnbull predicted nearly 40 years ago[33] that a crystalline nucleus is surrounded by a layer of molecules of liquid conforming as well as possible to the contours of the surface of the crystallites. This is the rationale for the increase in interfacial free energy with temperature (see above) and can account for differences between the CNT and the direct counts of KI ions in critical nuclei in the simulations. If we suppose that the Turnbull ordered liquid layer is counted by our criterion as solid (because it is ordered) and employ the relation we introduced some years ago[38] to estimate the fraction of molecules, F_s, in the surface of a quasispherical aggregate of N molecules, or

$$F_s = 3m(1 - 0.5m)^2 \quad (8)$$

where

$$m = [(4/3)\pi/N]^{1/3} \quad (9)$$

we can estimate the number of molecules that are core molecules (inside the ordered liquid layer at the surface). If we apply eq 8 to the direct counts of ordered KIs in critical nuclei we find 6, 8, and 13 KIs at 500, 550, and 580 K, respectively, and thereby obtain numbers that are in approximate agreement with those inferred via the CNT. The sizes of critical nuclei implied by the DIT are not greatly different from those implied by the CNT.

V. Concluding Remarks

In the molecular dynamics simulations of the freezing of small potassium iodide clusters, observed effects of temperature on nucleation rates, multiple nucleation events, and derived interfacial free energies were in the expected direction. Nucleation time lags, however, were not in the direction customarily seen but, nevertheless, were not anomalous in light of nucleation theory. Sizes of critical nuclei derived by a direct counting of ordered molecues in such nuclei bore scant relation to the sizes derived from the classical nucleation theory. If it were assumed, however, that the outer layer of molecules corresponded to the ordered layer of liquid molecules predicted by Turnbull but were falsely identified as belonging to the solid, then the disparity between the classical theory and simulation all but disappeared.

The size effects on nucleation rates deserve special comment. Smaller clusters exhibited higher rates. This phenomenon can be understood in terms of the higher Laplace pressure and the higher coefficient of diffusion in the smaller clusters, together with the strong tendency for nucleation to occur at the surface rather than in the interior of clusters. No clear-cut explanation of the latter phenomenon has yet been formulated.

Appendix

According to the classical nucleation theory (CNT), the nucleation barrier ΔG^* for a spherical nuclei is given by

$$\Delta G^* = 16\pi\sigma_{sl}^3/[3(\Delta G_v + w')^2] \quad (10)$$

where σ_{sl} is the interfacial free energy between solid and liquid, ΔG_v is the free energy change of freezing per unit volume of the solid, and w' is the work per unit volume of changing the surface area of liquid phase during the formation of the nucleus.

TABLE 6: Physical Properties of KI Adopted in the Calculation

property	value or expression	ref
T_m (K)	954	39
ΔH_{fus} (J/mol)	24 600	39
$C_p(l) - C_p(s)$ (J/mol K)	~15.4	31
V_{ms}(solid) (m^3/mol)	5.78×10^{-5}	31
V_{ml}(liquid) (m^3/mol)	6.78×10^{-5}	31
D (m^2/s), $(KI)_{500}$, $(KI)_{256}$	$9 \exp(-19\,000/R_JT)$	31
D (m^2/s), $(KI)_{108}$	$20 \exp(-20\,000/R_JT)$	31
σ_{vl} (J/m^2)	$0.1361 - 0.000\,06T$	40

The latter quantity for a drop of radius R is given by

$$w' = P_L(\rho_l - \rho_s)/\rho_l \tag{11}$$

where P_L is the Laplace pressure $2\sigma_{lv}/R$ inside the cluster and the ρ's are densities of liquid and solid.

In the diffuse-interface theory (DIT),[25-29] ΔG^* is given by

$$\Delta G^* = -4\pi\delta^3\Delta G_v\psi/3 \tag{12}$$

where δ is the thickness of the DIT layer and ψ is defined by[19]

$$\psi = [2(1+Q)H^{-2} - (3+2Q)H^{-1} + 1]/\eta \tag{13}$$

with $\eta = \Delta G_{fus}/\Delta H_{fus}$, $H = \eta(1+\zeta)$, $\zeta = w'/\Delta G_v$, and $Q = (1 - H)^{1/2}$.

The conventional formula used for the CNT prefactor is

$$A_{CNT} = 16(3/4\pi)^{1/3}(\sigma_{sl}/k_BT)^{1/2}D/V_m^{2/3}\Delta r^2 \tag{14}$$

where D is the coefficient of diffusion in the liquid; V_m is the volume of a molecule in solid; and Δr is the molecular jump distance from the liquid to the solid, usually taken to be $V_m^{1/3}$.

The DIT prefactor is[29]

$$A_{DIT} = \rho_1 O\Gamma Z \tag{15}$$

with $\rho_1 = 1/V_m$; $O = 4[4\pi(R_s^*)^3/(3V_m)]^{2/3}$; $\Gamma = 6D\Delta r^{-2}$; and $Z = \{V_m/[2\pi(R_s^*)^2]\}[-\Delta G_v(R_s^* - \delta/H)/(k_BT)]^{1/2}$, where R_s^* is the radius of the critical nucleus, which is calculated from $R_s^* = \delta(1+Q)H^{-1}$; Δr is, again, the jump distance from the liquid phase to the solid; and ΔG_v is the free energy difference per volume of solid between the supercooled liquid and the solid.

From the value of ΔG^* obtained from the observed nucleation rate, the quantities σ_{sl} and δ can be derived by applying the CNT and the DIT. All other parameters are known. The physical properties adopted for the analyses of the nucleation rates are listed in Table 6.

References and Notes

(1) Bartell, L. S.; Dibble, T. S. *J. Phys. Chem.* **1991**, *95*, 1159.
(2) Bartell, L. S. *J. Phys. Chem.* **1995**, *99*, 1080.
(3) Bartell, L, S In *Molecular Solid State: Theoretical Aspects and Computer Modeling*; Gavezzotti, A., Ed.; Wiley & Sons: Chichester, U.K., 1997; p 147.
(4) Bartell, L. S. *Annu. Rev. Phys. Chem.* **1998**, *49*, 43.
(5) Buckle, E. R. *Proc. R. Soc.* (*London*) **1960**, *A259*, 325.
(6) Buckle, E. R.; Ubbelohde, A. R. *Proc. R. Soc.* (*London*) **1960**, *A261*, 197.
(7) Huang, J.; Zhu, X.; Bartell, L. S. *J. Phys. Chem.* **1998**, *A102*, 2708.
(8) Bartell, L. S.; Huang, J. *J. Phys. Chem.* **1998**, *A102*, 8722.
(9) Deng, H.; Huang, J. *J. Solid State Chem.* **2001**, *159*, 10.
(10) Ma, M.; Lu, W.; Huang, J. *J. Solid State Chem.*, in press.
(11) Anastasiou, N.; Fincham, D. *MDIONS*; CCP5 Program Library; SERC Daresbury Laboratory: Daresbury, U.K.
(12) Pathak, P. D.; Pandya, N. V. *Indian J. Phys.* **1960**, *34*, 416.
(13) Born, M.; Mayer, J. E. *Z. Phys.* **1932**, *75*, 1.
(14) Huggins, M. L.; Mayer, J. E. *J. Chem. Phys.* **1933**, *1*, 643.
(15) Huggins, M. L. *J. Chem. Phys.* **1937**, *5*, 643.
(16) Tosi, M. P.; Fumi, F. *J. Phys. Chem. Solids* **1964**, *25*, 45.
(17) Kinney, K. E.; Xu, S.; Bartell, L. S. *J. Phys. Chem.* **1996**, *100*, 6935.
(18) Chushak, Y. G.; Bartell, L. S. J. *Phys. Chem.* **2000**, *A104*, 9328.
(19) Chushak, Y. G.; Santikary, P.; Bartell, L. S. *J. Phys. Chem.* **1999**, *A103*, 5644.
(20) Bartell, L. S. *J. Phys. Chem. A*, manuscript submitted.
(21) Wu, D. In *Solid State Physics*; Ehrenreich, H., Spaepen, F., Eds; Academic Press: New York, 1997; Vol. 50, p 38.
(22) Greer, A. L.; Kelton, K. F. *J. Am. Ceram. Soc.* **1991**, *74*, 1015.
(23) Turnbull, D.; Fisher, J. C. *J. Chem. Phys.* **1949**, *17*, 71.
(24) Buckle, E. R. *Proc. R. Soc.* (*London*) **1961**, *A261*, 189.
(25) Granasy, L. *Europhys. Lett.* **1993**, *24*, 121.
(26) Granasy, L. *J. Non-Cryst. Solids* **1993**, *162*, 301.
(27) Granasy, L. *Mater. Sci. Eng.* **1994**, *A178* 121.
(28) Granasy, L. *J. Phys. Chem.* **1995**, *99*, 14183.
(29) Granasy, L.; Igloi, F. *J. Chem Phys.* **1997**, *109*, 3634.
(30) Kelton, K. F.; Greer, A. L.; Thompson, C. V. *J. Chem. Phys.* **1983**, *79*, 6261.
(31) Huang, J.; Bartell, L. S. *J. Mol. Struct.* **2001**, *567*, 145.
(32) Kashchiev, D.; Verdoes, D.; van Rosmalen, G. M. *J. Cryst. Growth* **1991**, *110*, 373.
(33) Turnbull, D. In *Physics of Non-Crystalline Solids*; Prins, J., Ed; North-Holland: Amsterdam, 1964; p 4.
(34) Turnbull, D. *J. Chem Phys.* **1952**, *20*, 411.
(35) Huang, J.; Bartell, L. S. *J. Phys. Chem.* **1995**, *99*, 3924.
(36) Compare Figure 8, ref 2; Figure 5.2, ref 3; and Figure 6, ref 4.
(37) Turnbull, D. *J. Appl. Phys.* **1950**, *21*, 1022.
(38) Huang, J.; Bartell, L. S. *J. Phys. Chem.* **1994**, *98*, 4543.
(39) Dworkin, A. S.; Bredig, M. A. *J. Phys. Chem.* **1960**, *64*, 269.
(40) Sato, Y.; Ejima, T.; Fukasawa, M.; Kenji, A. *J. Phys. Chem.* **1990**, *94*, 1991.